Bimodal and unimodal radial growth of Mediterranean oaks along a coast-inland gradient

Jan Tumajer [a],[*], Xavier Serra-Maluquer [b],[c], Antonio Gazol [b], Ester González de Andrés [b], Michele Colangelo [b], Gabriel Sangüesa-Barreda [d], José Miguel Olano [d], Vicente Rozas [d], José Ignacio García-Plazaola [e], Beatriz Fernández-Marín [f], J. Bosco Imbert [g], Lluís Coll [h], Aitor Ameztegui [h],[i], Josep Maria Espelta [j], Arben Q. Alla [k], Filipe Campelo [l], J. Julio Camarero [b]

[a] *Department of Physical Geography and Geoecology, Faculty of Science, Charles University, Albertov 6, Prague 12843, Czech Republic*
[b] *Instituto Pirenaico de Ecología (CSIC), Avda. Montañana 10005, Zaragoza 50009, Spain*
[c] *Departamento de Biología Vegetal y Ecología, Universidad de Sevilla, Apdo.1905, Sevilla 41080, Spain*
[d] *EiFAB-iuFOR, Universidad de Valladolid, Campus Duques de Soria, Soria 42004, Spain*
[e] *University of the Basque Country, (UPV), Leioa, Spain*
[f] *University of La Laguna, San Cristóbal de La Laguna, Spain*
[g] *Institute for Multidisciplinary Research in Applied Biology IMAB, Public University of Navarre, Pamplona, Navarra, Spain*
[h] *Department of Agriculture and Forest Engineering (EAGROF), University of Lleida, Lleida, Spain*
[i] *Joint Research Unit CTFC – AGROTECNIO, Solsona, Spain*
[j] *CREAF, Bellaterra, Spain*
[k] *Fakulteti i Shkencave Pyjore, Universiteti Bujqësor i Tiranës, Tirana 1029, Albania*
[l] *Centre for Functional Ecology, Department of Life Sciences, University of Coimbra, Calçada Martim de Freitas, Coimbra 3000-456, Portugal*

ARTICLE INFO

ABSTRACT

Wood formation during the growing season is shaped by the intra-annual variability of climatic conditions. In the Mediterranean, the cambial activity is seasonally constrained by winter low temperature and summer drought, resulting in bimodal growth patterns. Although bimodal growth is an ecologically important adaptation of woody species to seasonally dry environments, its variability across space and among species remains unclear. We combined direct monitoring of intra-annual radial growth using dendrometers and xylogenesis micro-sampling with indirect wood formation modeling to assess growth bimodality for two coexisting oak species across six sites in North-Eastern Spain. We focused on species with two contrasting life strategies, evergreen with diffuse-porous wood (*Quercus ilex*) and winter deciduous with ring-porous wood (*Q. faginea/Q. pubescens*). Study sites spanned from oceanic areas with high autumn precipitation to dry continental inland regions. We hypothesized that growth bimodality reflects the interaction between local precipitation patterns and species-specific traits. Our results revealed cambial activity in autumn after summer quiescence across the entire region and for both oak species. However, growth bimodality and the relative contribution of the autumn growth peak to the total annual growth was geographically structured and species-specific. Growth was unimodal under continental and Atlantic conditions. By contrast, growth bimodality was significant along the Mediterranean coast, where precipitation showed a bimodal pattern. Moreover, evergreen *Q. ilex* showed more growth bimodality compared with deciduous *Q. faginea/Q. pubescens* at Mediterranean sites. Different intra-annual distribution of radial growth could facilitate coexistence of both oak species through temporal niche partitioning. The growth bimodality helps to compensate for reduced growth in summer by autumn cambial resumption and, therefore, the differences in its intensity between sites and species may determine divergent responses of forest ecosystems to ongoing climate change.

1. Introduction

Forest ecosystems globally sequester about 40% of total anthropogenic emissions of CO_2 (Pan et al., 2011) and, hence, play an important role in mitigating climate change (Peñuelas et al., 2009). Understanding how tree growth is sensitive to climatic variations on different spatial and temporal scales is essential for forecasting future growth dynamics and forest productivity (Soja et al., 2007). In seasonal climates, the timing and rate of wood formation during the year is determined by seasonal variability of temperature (Delpierre et al., 2019), photoperiod (Huang et al., 2020), soil moisture availability (Zweifel et al., 2021) or their interactions. The overall influence of temperature and water availability on radial growth may vary across climatic zones (Babst et al., 2019) and, consequently, intra-annual patterns of wood formation could diverge across species distribution ranges (Delpierre et al., 2019; Tumajer et al., 2021a). This challenges the understanding of intra-annual growth dynamics across regions subjected to high climate variability.

Approximately 7% of the global land surface experiences bimodal precipitation patterns with two precipitation maxima during the year (Knoben et al., 2019). Many woody species in seasonally-dry regions, such as the Mediterranean biomes, split their radial growth into two distinct moist periods in spring and autumn with no or limited growth during dry summer and cold winter (Cherubini et al., 2003; Mitrakos, 1980). This results in bimodal or multimodal intra-annual growth patterns that are frequently observed across Mediterranean (Balzano et al., 2018; Camarero et al., 2010), semi-arid (Ziaco and Biondi, 2018; Morino et al., 2021) and dry continental regions (Popkova et al., 2018). The intra-annual growth dynamics of coexisting tree species might differ between unimodal and bimodal depending on the ability of each species to reactivate cambial activity after summer quiescence. In the Mediterranean, growth bimodality tends to be stronger in coniferous (Camarero et al., 2010) than in diffuse-porous broadleaved species (Campelo et al., 2021), while the growth of ring-porous broadleaves is usually unimodal (Martínez-Sancho et al., 2021; Vieira et al., 2022). Tree species with a bimodal growth benefit from autumn growth reactivation by lengthening the growing season leading to larger annual increments compared with species with a unimodal growth restricted to the spring wet period (Zhang et al., 2020). By contrast, species with unimodal growth often show early spring onset of growing season compensating for the lack of autumn growth (Sass-Klaassen et al., 2011). Indeed, different levels of growth bimodality might contribute to species coexistence by temporal niche partitioning through uncoupled phenology during the growing season (Huang et al., 2019). In addition to variability between coexisting species, the frequency and intensity of bimodality tends to vary among years (Zhang et al., 2020), microsites (Campelo et al., 2018) and even between individual trees of the same species (Zalloni et al., 2016). Although growth bimodality is recognized as an ecologically important adaptation to seasonally dry conditions (Mitrakos, 1980), there is limited understanding about how the bimodality varies across space and time. Such knowledge gap should be filled, since radial growth limitation by low soil moisture is increasing in many forested ecosystems as climate warms (Babst et al., 2019).

Spatial and temporal patterns of intra-annual growth dynamics might be described using direct and indirect approaches. Dendrometers (Drew and Downes, 2009) and xylogenesis monitoring (Rathgeber et al., 2016) represent direct methods based on the intra-annual measurement of stem radius increment and xylem cell production, respectively. Although direct empirical data are essential (Cuny et al., 2015), currently available datasets on intra-annual growth are often spatially scarce and cover short periods (but see Zweifel et al., 2021). To compensate for these limitations, intra-annual growth dynamics can be simulated using process-based models of wood formation. They represent approximations of the current state of knowledge about the internal and external processes shaping radial growth (Eckes-Shephard et al., 2022). Although process-based models can overcome some limitations

related to the lack of dendrometer and xylogenesis data in specific sites and periods, they represent just an approximation of the real growth patterns (Evans et al., 2006) and might be prone to temporal non-stationarity (Wilmking et al., 2020). Accordingly, a combination of empirical and simulated data is desirable to assess the limitations of each approach and to better understand the multiple sources of intra-annual growth variability.

In this study, we combined available datasets of xylogenesis monitoring and dendrometers with process-based modeling to describe regional variability in growth bimodality for two groups of coexisting Mediterranean oak species with different life strategies (evergreen *Quercus ilex* L. and deciduous *Quercus faginea* Lam. / *Quercus pubescens* Willd.). To do so, we established six sites and assembled 12 species-specific growth chronologies in North-Eastern Spain where precipitation exhibits pronounced bimodality (Knoben et al., 2019) and, therefore, growth bimodality is expected. For each site and species, we calibrated the Vaganov-Shashkin model (further abbreviated VS-model; Vaganov et al., 2006) simulating daily growth dynamics between 1980 and 2017, and monitored intra-annual growth using band dendrometers and xylogenesis microcores during a single growing season. We employed graphical and statistical approaches on all datasets to describe the level of growth bimodality for each site and species. We assumed that (i) growth bimodality as an adaptation to bimodal precipitation will be the most prominent at sites close to the Mediterranean coast (Pacheco et al., 2018), and (ii) the evergreen *Q. ilex* will show more evident bimodal pattern compared with the deciduous *Q. faginea/Q. pubescens* in accordance with previous phenological observations showing spring and facultative autumn growth peaks in the former species and a marked spring growth peak in the later species (Alday et al., 2020; Camarero et al., 2021; Campelo et al., 2018; Montserrat-Martí et al., 2009).

2. Material and methods

2.1. Study area and study species

We selected six sites where *Q. ilex* and *Q. faginea/Q. pubescens* coexist in North-Eastern Spain (Fig. 1a). Sites were distributed along a NW-SE gradient from the winter-spring moist Atlantic coast (Tertanga site, TE) to the mild Mediterranean coast (Collserola and Oliola sites, CO and OL) with dry summers and wet autumns (Knoben et al., 2019). Continental sites with cold winters and a short growing season (Soria site, SO) and semi-arid sites (Alcubierre site, AL) were also considered. Sansoain site (SA) showed intermediate climate conditions between coastal and interior sites. The mean annual precipitation ranged from 389 to 989 mm, and mean annual temperatures ranged from 10.8 to 16.2°C (Fig. 1c). In all sites the period from July to August was dry with increasing summer precipitation deficit from NW (Tertanga) to SE (Collserola). Precipitation peaked in spring at all sites except Collserola with autumn precipitation maximum.

Quercus ilex is an evergreen oak with diffuse to semi-ring porous wood with a wide distribution across the western Mediterranean basin (Fig. 1b). This species presents a high phenotypic variability in morphological traits including fine roots (Coll et al., 2012), xylem anatomy and leaf size (Peguero-Pina et al., 2014). Two subspecies are often considered, one fast-growing with bigger leaves (*Quercus ilex* subsp. *ilex*) occurring in the two coastal sites (Tertanga, Collserola), and one slow-growing with smaller and thicker leaves (*Quercus ilex* subsp. *ballota*) occurring in the other four sites. *Quercus faginea* is a winter deciduous oak with ring porous wood distributed across the Iberian Peninsula and North Africa. In North-Eastern Spain, it can hybridize with *Quercus pubescens* (= *Q. humilis* Mill.). The leaf and acorn characteristics corresponded to *Q. faginea* in all sites except Collserola, where traits were closer to *Q. pubescens*. Therefore, we refer to these taxa as *Q. faginea/Q. pubescens*. Where *Q. ilex* and *Q. faginea/Q. pubescens* coexist, the deciduous species sprout and start leaf development in
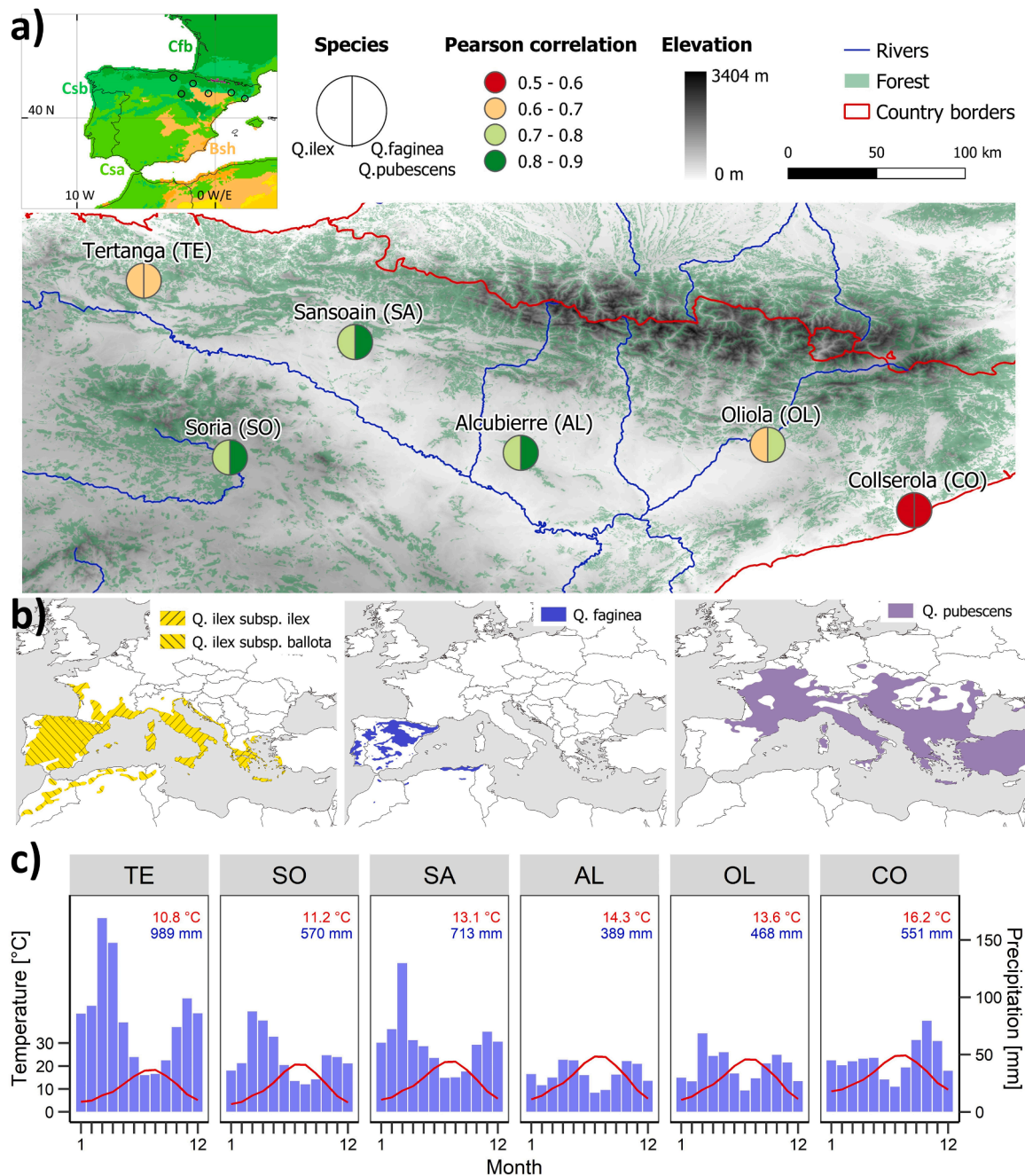
Fig. 1. Geographic position of the study sites in the Northern Spain (a), distribution range of the oak species under the study (b) and site climatic diagrams (c). The color scale of symbols in (a) indicates correlation coefficients between simulated and observed tree-ring width chronologies for evergreen (*Q. ilex*) and deciduous (*Q. faginea/Q. pubescens*) oak species. All correlations are statistically significant ($p < 0.01$). Underlying colors of the inset in (a) represent Köppen-Geiger climate classification (Bsh = hot semi-arid climate, Csa = hot-summer Mediterranean climate, Csb = warm-summer Mediterranean climate, Cfb = temperate oceanic climate). Mean monthly temperatures (red lines) and mean monthly precipitation totals (blue bars) during the period 1980–2017 are shown in (c). Numbers in top-right corner of (c) indicate mean annual temperature and annual precipitation totals. Forest distribution in (a) is according to CORINE database and species distribution ranges in (b) according to Caudullo et al. (2017).

spring about two weeks before the evergreen species (Fig. S1; Montserrat-Martí et al., 2009). *Quercus ilex* is more tolerant to soil water shortage than *Q. faginea/Q. pubescens* which tend to dominate in mesic sites with deeper or wetter soils (Caudullo et al., 2017). All study sites were secondary forests where most oak trees were relatively young (30–70 years) and colonized former croplands and grasslands.

2.2. Growth monitoring and climatic data

To characterize oak growth on intra- and inter-annual scales, we monitored stem radius variation using dendrometers, extracted wood microcores for xylogenesis assessment, and, finally, we sampled increment cores to measure annual tree-ring widths. In total, we acquired dendrometer and xylogenesis data for 120 and 40 trees, respectively, and cored 187 trees. We also measured the diameter at breast height of cored and monitored individuals (Table S1).

To monitor intra-annual growth dynamics, we installed manual band dendrometers (DB20, EMS, Brno, Czech Republic) on ten individuals per species and site in winter 2007–2008. We removed the outer dead bark before installing dendrometers to reduce the bias due to its hygroscopic

effects. The reading of dendrometers was performed biweekly with a precision of 0.1 mm during 2008 in all sites. In 2009, dendrometers were maintained in four sites (Tertanga, Soria, Sansoain, Alcubierre) and two sites (Soria, Alcubierre) were still monitored in 2010. We converted stem girth recorded by dendrometers into stem radius assuming a circular cross-section of the stem. We subtracted stem radius at the beginning of calendar year from each observation to estimate a width of forming tree ring at each date.

In addition to dendrometers, we monitored xylogenesis during the 2008 growing season at four study sites (Tertanga, Soria, Sansoain and Alcubierre). Biweekly, we extracted microcores with a diameter of 2 mm from the stem of five individuals per species and site using the Trephor tool (Rossi et al., 2006). Samples were extracted following a spiral along the stem and separated by at least 10 cm from the previous sampling. The microcores were processed using standard laboratory techniques: paraffin embedding of samples, cutting them on a sliding microtome (15–20 μm thickness) and staining the sections to enhance the contrast between cell walls and lumens (Gärtner and Schweingruber, 2013). Next, we observed each microsection using the optical microscope and measured the width of the developing tree ring to a precision of 0.001 mm.

To assess growth variability between years, we extracted increment cores from 14 to 20 individuals per site and species during late 2017 using Presslers increment borers. Cores were air-dried, glued into wooden holders and their surface was polished to enhance the visibility of xylem cellular elements, particularly tree-ring boundaries. Next, we measured the tree-ring widths of each sample up to the precision of 0.001 mm using Lintab-TSAP measuring device. Each measured tree-ring width series was visually and statistically cross-dated to identify possible missing and false rings (Holmes, 1983). We removed biological trends from the tree-ring width series by fitting a spline with a 50% frequency cut-off at 20 years to each series and removed temporal autocorrelation by pre-whitening using ARMA models (Cook and Peters, 1981). Finally, we averaged individual series per site and species into 12 pre-whitened residual chronologies (six site chronologies for *Q. ilex* and six site chronologies for *Q. faginea/Q. pubescens*). All chronologies were trimmed to cover 1980–2017 which is the best replicated period common to all sites.

For each site, we obtained daily mean air temperature and precipitation data from E-OBS gridded database with 0.1° spatial resolution (version 25.0.; Cornes et al., 2018). The climatic data were acquired for the period between 1st January 1980 and 31st December 2017.

2.3. Regional master tree-ring width chronology

Because the North-Eastern Spain is characterized by a drought-driven growth of trees (Gazol et al., 2018; Zalloni et al., 2016), we expected similarities in growth patterns and climate-growth responses among sites and species. Accordingly, we assembled two regional species-specific 'master' tree-ring width chronologies, climate series, dendrometer and xylogenesis datasets to characterize overall regional growth patterns. To do so, we first performed two principal component analyses (PCA) on the variance-covariance matrix of the site ring-width chronologies for each species. The master tree-ring width chronologies were defined as the first principal components of the PCA. Contributions of each site chronology to the first principal component were used as weights to determine mean series of temperature, precipitation, xylogenesis and dendrometer data relevant to master chronologies.

2.4. Process-based modelling of intra-annual growth dynamics

To complement single year (2008) of radial growth observations with biweekly resolution, we employed the Vaganov-Shashkin process-based model of tree-ring formation (Vaganov et al., 2006) to simulate daily growth variability for each site and species during entire 1980–2017 period. The VS-model is a climate-driven sink-oriented model of moderate complexity initially developed for conifers from cold biomes, but successfully used across broad spatial gradients and for different species (Eckes-Shephard et al., 2022). Inputs include daily resolved temperature, precipitation and site latitude. VS-model assumes that the daily growth rate of an idealized tree is driven by temperature, soil moisture and photoperiod of a specific day. The daily soil moisture is determined by inbuilt hydrological submodel from daily temperatures and precipitation totals considering processes of interception, evaporation, transpiration, surface runoff, soil infiltration and snow dynamics. In the first step, the model determines unitless daily partial growth rates to temperature (GrT) and soil moisture (GrM) using non-linear response functions of a specific climatic variable. GrT and GrM indicate relative suitability of temperature and soil moisture for radial growth with higher values representing better conditions for growth. The model assumes, that the climatic variable with a dominant limiting effect (i.e., the lower of partial growth rates) fully controls radial growth of a given day. Therefore, the lower of partial growth rates is scaled by the daily photoperiod to produce an integral growth rate (Gr), which is a proxy of daily radial growth rate. Annual growth rate is defined as a standardized sum of daily integral growth rates during a specific year (Tychkov et al., 2019).

We parameterized the VS-model for each of our 14 chronologies (12 site- and species-specific chronologies and two master regional chronologies). For each chronology, we provided site-specific climatic data as input into the model and tuned the model parameters to maximize the correlation between simulated and observed chronologies using a graphical tool VS-Oscilloscope (ver. 1.37; Shishov et al., 2016). To reduce the risk of overfitting, we set parameters related to plant water balance, growth phenology and the response of growth to high soil moisture to be constant across all sites and species (see also Touchan et al., 2012; Tumajer et al., 2021b). Moreover, we considered initial soil moisture as a spatially-explicit parameter to be constant for both species from the same site. Accordingly, we permitted only ten parameters to vary between coexisting species and one additional parameter to vary among sites but not between species (Table S2). Because of the short common span of our chronologies (38 years) we were not able to assess the model stationarity using a calibration-verification exercise on independent sufficiently-long subperiods. To overcome this limitation, we calibrated models and interpreted their results for the best-replicated common period (1980 to 2017). Consequently, our models should be considered the best fits for this period but their stationarity outside the calibration interval is not validated (Wilmking et al., 2020).

In addition to correlating simulated and observed tree-ring width chronologies, we compared the simulated pattern of daily integral growth rates in 2008–2010 against dendrometer and xylogenesis data to validate the modelled intra-annual progress of tree-ring formation. To do so, we first averaged dendrometer and xylogenesis observations from individual trees to site and species level. Next, we plotted simulated and observed proportions of tree-ring formed at each day of the year to visually assess their similarity. To overcome different units of observed (mm) and simulated (unitless) ring widths we standardized all datasets by the tree-ring width simulated or observed at the end of the year (i.e., the final annual tree-ring width = 100%). We smoothed dendrometer, xylogenesis and simulated intra-annual growth dynamics using Generalized Additive Models (GAM) of a Gaussian family to aid their visual comparison. We considered all declines of stem radius recorded by dendrometers between two consecutive periods as a consequence of stem shrinkage due to tree water deficit, while increments between consecutive periods were treated as stem radial growth (Zweifel et al., 2016). Accordingly, before fitting GAM models, we replaced the values of stem radius during shrinkage phases with a previous maximum of the stem radius.

2.5. Quantification of bimodality in the simulated growth patterns

We plotted daily integral growth rates (Gr) averaged for the entire

1980–2017 period to visually characterize the mean simulated growth dynamics of each chronology. To statistically quantify the shape of the distribution of growth rates, we calculated skewness and kurtosis of simulated integral growth rates smoothed using GAM for each species, site and year. The kurtosis reflects the relative dominance of local peaks in the distribution with positive/negative values indicating sharp peaks/narrow plateaus (i.e., 'spikiness/flatness'). The skewness is sensitive to the position of the global optimum concerning the center of the distribution. Positive/negative values of skewness indicate shifts of global optimum to the early/late (i.e., left/right) part of the distribution. We expected that bimodal and multimodal Mediterranean growth patterns will be characterized by high kurtosis due to the occurrence of abrupt growth and quiescence episodes during moist and dry days, respectively. We also assumed that the skewness would indicate the relative importance of spring and autumn growth periods for annual growth. We plotted boxplots of skewness and kurtosis of individual years to compare the level of bimodality between sites. We also compared mean values of each statistics between *Q. ilex* and *Q. faginea/Q. pubescens* from the same site using paired Wilcoxon sign tests.

2.6. Climatic drivers of radial growth

We used simulated daily partial growth rates to identify the most important climatic growth-limiting factor for each day of the year. Based on the daily values of Gr, GrT and GrM, the VS-model distinguishes between limitations by high/low temperatures (GrT < GrM), high/low soil moisture (GrT > GrM), climatically unlimited (optimal) growth (GrT = GrM = 1) and no growth during dormancy or quiescence (Gr = 0; see Tumajer et al., 2021b for further details). We plotted the distribution of days with different climatic limitations into the matrix to visually highlight their shifts during the year and between years.

To complement the simulations produced by the VS-model, we also calculated linear climate-growth correlations between observed chronologies and daily climatic data. We calculated mean temperatures and precipitation sums for all possible periods with duration from 30 to 90 days between 1st January and 31st December. Next, we calculated Pearson correlation coefficients between aggregated climatic data and chronologies. Individual correlations were plotted into the matrix to visually highlight their intra-annual shifts.

All steps of statistical processing and visualization of the data were performed in R (R Core Team, 2021) using packages 'dplR' (processing
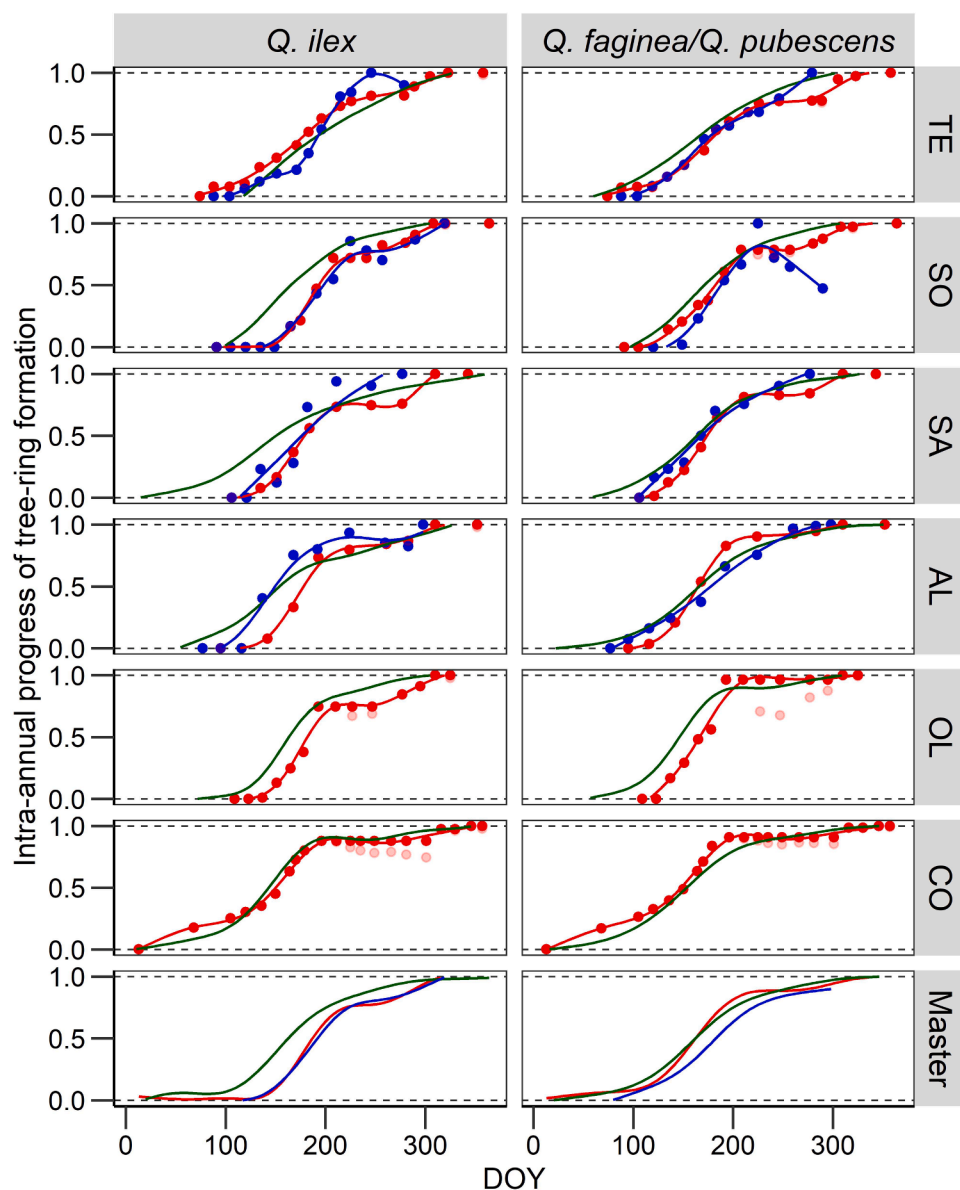

Fig. 2. Comparison of intra-annual growth dynamics observed by dendrometers (red lines and points), determined from xylogenesis samples (blue lines and points) and the simulations produced by the VS-model (green lines) for 2008 and each site and species. Y-axes shows the proportion of the tree-ring that was formed during specific day of the year with all variables standardized by their annual maximum (i.e., the moment when maximum ring width was achieved during the year has a value of 1.0 on y-axes). Points refer to days when the tree-ring formation was observed using xylogenesis and dendrometers, lines are GAM fits through observed and simulated data. Transparent red points show stem diameter recorded by dendrometer, full red points show stem radial increment (i.e., stem diameter without the effect of stem shrinkage due to tree water deficit). See Figs. S3 and S4 for results from the years 2009 and 2010, Fig. 1 for codes of each site, and Fig. S2 to aid a direct visual comparison of growth patterns between sites. DOY = day of year.

of tree-ring data; Bunn, 2008), 'e1071' (skewness and kurtosis; Meyer et al., 2021), 'gam' (GAM models; Hastie, 2022), 'dendrotools' (climate-growth correlations; Jevšenak and Levanič, 2018) and 'ggplot2' (charts' plotting; Wickham, 2009).

3. Results

The dendrometer data for 2008 revealed spring growth peak in all sites and species, followed by a summer growth quiescence or even stem shrinkage starting around DOY 200 (day of the year; Figs. 2, S2). The quiescence was followed by an optional secondary growth peak in autumn, whose timing and intensity, however, varied across sites. The pronounced summer stem shrinkage and autumn growth peak were recorded by dendrometers at the Mediterranean and some inland sites whilst autumn growth diminished towards Atlantic sites. Autumn growth peaks were visually more evident in *Q. ilex* compared with *Q. faginea/Q. pubescens*, mainly at Collserola, Oliola, Alcubierre and Sansoain sites. The dendrometers recorded pronounced growth bimodality also at Soria and Sansoain sites during 2009, but not during 2010 (Figs. S3 and S4). The autumn growth period in 2008 was visually more important in dendrometer observations compared with xylogenesis data (Figs. 2, S2).

The tree-ring width chronologies simulated by the VS-model were highly correlated with all 12 site- and species-specific chronologies ($r = 0.55$–0.85; $p < 0.01$; Fig. 1a). The correlations between observed and simulated chronologies were higher for *Q. faginea/Q. pubescens* compared with *Q. ilex* at all sites except Collserola, where the values were similar for both species. The correlations were higher for inland sites (Soria, Sansoain, Alcubierre, Oliola) compared with coastal sites (Tertanga, Collserola; Fig. 1a). The regional master chronologies explained 44% and 49% of the total variability between site chronologies for *Q. ilex* and *Q. faginea/Q. pubescens*, respectively (Fig. S5) and were significantly correlated with the simulations produced by the VS-model ($r = 0.82$–0.83; $p < 0.01$; Fig. S6). Calibrated values of the VS-model parameters are listed for each chronology in Table S2.

Simulated intra-annual growth patterns for 2008 followed those observed using dendrometers with early-spring cambial reactivation, a peak of growth rate in late spring followed by a growth decline through summer but maintaining or even increasing growth till late autumn (Figs. 2, S2). Summer was the period with the most important deviations between simulated and observed intra-annual growth patterns. Specifically, the model did not fully reflect observed growth quiescence, mainly at Soria and Sansoain sites. Over the entire 1980–2017 period, the mean intra-annual growth pattern showed the gradient from visually right-skewed unimodal with stable summer growth at Tertanga Atlantic site towards bimodal patterns with reduced summer growth and secondary autumn peak at Oliola and Collserola Mediterranean sites (Fig. 3). An evident bimodal growth pattern with summer growth quiescence and subsequent autumn growth reactivation was simulated only for *Q. ilex* at the Collserola site.

Values of skewness and kurtosis were calculated for simulated daily growth rates to numerically quantify the shape of growth rates' distribution for each site, species and year. The statistics were higher for sites located near the Mediterranean Sea (*Q. ilex* at Collserola, both species at Oliola) compared with inland and Atlantic sites (Fig. 4). For inland and Atlantic sites, the values of both statistics were similar between species and close to the values obtained for regional master chronologies. At the Mediterranean sites, by contrast, both skewness and kurtosis were usually significantly higher compared with master chronologies. Between-species differences were the most pronounced at Collserola and Oliola Mediterranean sites and Soria inland site, where values of skewness and kurtosis were significantly higher for *Q. ilex* compared with *Q. faginea/Q. pubescens*.

Climate-growth responses derived from the VS-model and climate-growth linear correlations highlighted a drought limitation of all sites. The VS-model classified the majority of days as dry or warm with only
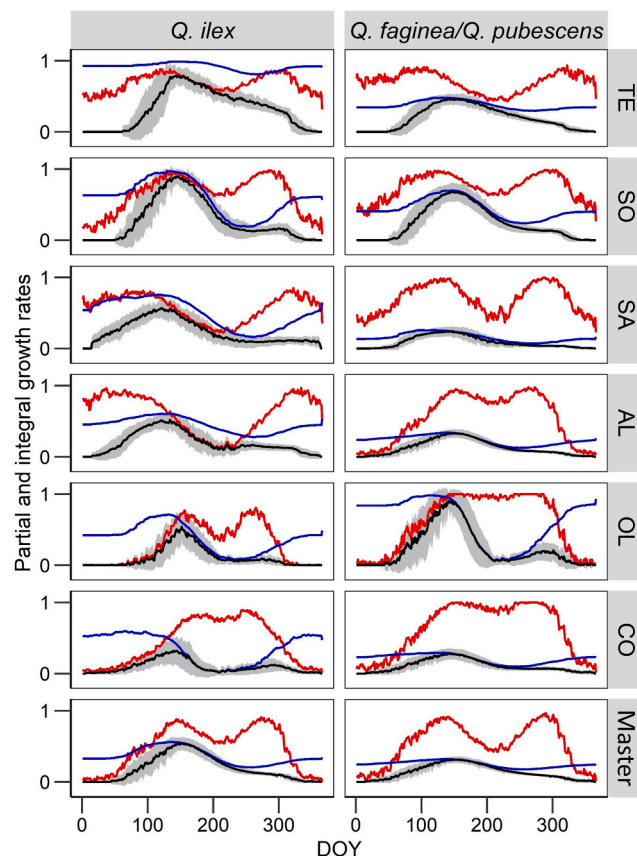

Fig. 3. Mean intra-annual patterns of daily partial growth rates to temperature (red), partial growth rates to soil moisture (blue) and integral growth rates (black) for each chronology simulated by the Vaganov-Shashkin model for the period 1980–2017. The buffer around lines for integral growth rates indicates ± standard deviation between individual years. See codes of each site in Fig. 1. DOY = day of year.
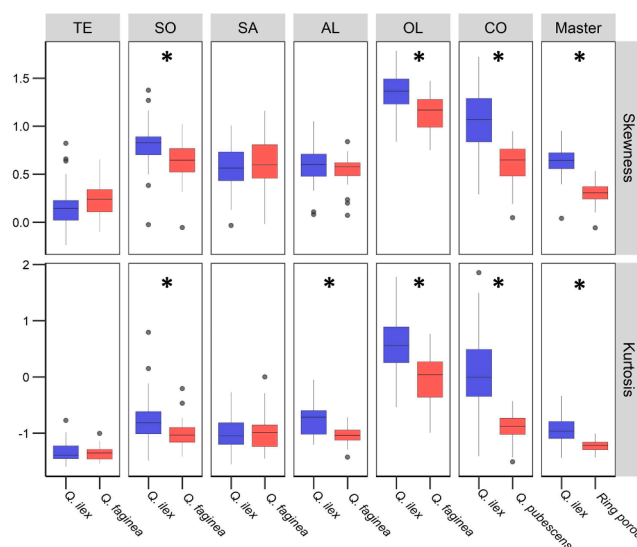

Fig. 4. Boxplots of skewness and kurtosis of smoothed simulated intra-annual growth rates for each year from 1980 to 2017 and for each site and master chronology (diffuse vs ring-porous oak species). Asterisks mark sites with significant ($p < 0.01$) differences between species indicated by paired Wilcoxon signed tests. See codes of each site in Fig. 1.

rare occurrence of cold or climatically optimal days at some sites during early spring (Fig. 5). Climate-growth correlations confirmed the positive effect of spring precipitation and the negative effect of summer temperature on growth at most sites (Fig. S7). Autumn climate-growth correlations were mostly non-significant for both temperature and precipitation.

4. Discussion

Our results highlight the importance of autumn cambial growth in seasonally dry areas such as North-Eastern Spain (Camarero et al., 2010; Mitrakos, 1980). A systematic spatial gradient was observed in dendrometer data and confirmed by simulations with growth unimodality prevailing at Atlantic sites, while at sites towards the Mediterranean coast the bimodal growth was more prevalent. Both simulated and observed growth bimodality was more evident for *Q. ilex* compared with *Q. faginea/Q. pubescens* mainly at the Mediterranean sites in agreement with previous phenological observations (Camarero et al., 2021; Montserrat-Martí et al., 2009). Although drought limited cambial activity at all study sites, we report systematic differences in radial growth among

species and across sites with possible implications for the divergent response of forest ecosystems to ongoing climate change.

4.1. Spatial variability in simulated and observed intra-annual growth patterns

The simulated and observed growth patterns showed a systematic gradient from the Atlantic to Mediterranean coasts. While the simulated intra-annual growth was right-skewed unimodal and dendrometers revealed mostly continuous radial growth during summer at Tertanga Atlantic site, summer stem shrinkage and autumn growth reactivation became more prominent towards Oliola and Collserola sites close to the Mediterranean coast (Figs. 2, S2–S4). This confirms that bimodal growth features a systematic variability in space (Camarero et al., 2010; Campelo et al., 2018). A growth bimodality is linked to an abrupt termination of a summer drought stress by sufficient autumn precipitation (Morino et al., 2021; Touchan et al., 2012; Ziaco and Biondi, 2018). Indeed, growth bimodality tends to be amplified in areas with bimodal precipitation and summer drought stress which are close to the Mediterranean coast (Fig. 1c; Knoben et al., 2019). Although the sites close to
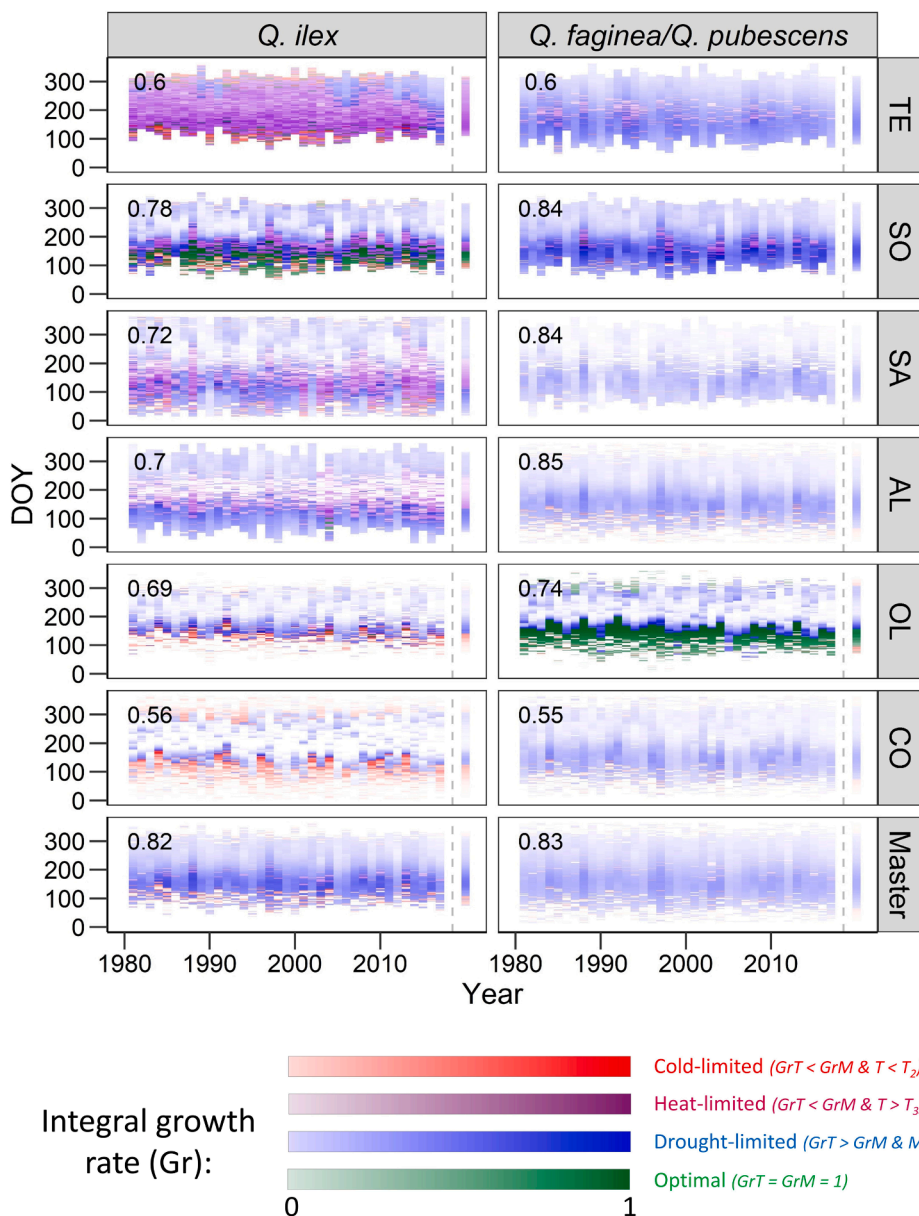

Fig. 5. Matrices of simulated daily integral growth rates for each year of chronology. The color intensity indicates simulated integral growth rate with values close to 0/1 representing conditions of strong/mild climatic limitation and low/high daily growth rate. The color refers to dominant climatic limiting factors: drought (blue), high temperature (purple), low temperature (red), optimal growing conditions (green), winter dormancy and summer quiescence (white, Gr = 0). The right-most column of the matrix shows the mean values of daily integral growth rates over the common period (1980–2017). Numbers in the top-left corner indicate Pearson correlations between simulated and observed chronologies. All correlations are statistically significant with $p < 0.01$. Abbreviations: T = daily temperature; M = daily soil moisture; GrT/GrM = simulated partial growth rates to temperature/soil moisture. See codes for each site in Fig. 1. DOY = day of year.

the Atlantic coast also experience bimodal precipitation pattern, the summer drought period is short and less intense, resulting in continuous summer growth and unimodal growth pattern (Fig. 3). Consequently, our observations and simulations support a high intensity of bimodality reported from Mediterranean coastal areas with less continental, maritime climate (De Micco et al., 2016; Martínez-Sancho et al., 2021; Pacheco et al., 2018; Prislan et al., 2016; Vieira et al., 2017).

4.2. Different intra-annual growth patterns between coexisting oaks

Between-species differences were the most important at Mediterranean and some of inland sites, where *Q. ilex* showed stronger bimodality compared with coexisting *Q. faginea/Q. pubescens* (Figs. 2, 4, S2). In Mediterranean coastal areas, the dominant *Q. ilex* subsp. *ilex* is adapted to resume growth in response to autumn precipitation resulting in additional xylem layers formed at the end of the ring (Campelo et al., 2007). Accordingly, simulated growth patterns had higher kurtosis and skewness for *Q. ilex* compared with *Q. faginea/Q. pubescens* mainly at Collserola and Oliola Mediterranean sites. These systematic differences between both oak species agreed with previous observations. Specifically, while the growth was reported to be rather right-skewed unimodal in Iberian deciduous ring-porous oaks (Martínez-Sancho et al., 2021; Vieira et al., 2022), the evergreen diffuse-porous *Q. ilex* is known for its facultative bimodality (Campelo et al., 2018). *Quercus ilex* tends to shift between right-skewed unimodal and bimodal growth patterns depending on late-summer and early-autumn climatic conditions (Campelo et al., 2021, 2007). Nevertheless, observed and simulated growth bimodality of *Q. ilex* is still substantially lower compared with bimodality of many Mediterranean conifers, such as *Pinus halepensis* Mill. and *Juniperus thurifera* L. (Campelo et al., 2021; de Luis et al., 2007; Tumajer et al., 2021b) and, indeed, this evergreen oak should be considered as moderately-bimodal among Mediterranean forest species.

Observed and simulated differences between species might reflect different phenological and physiological adaptations to drought stress. Ring-porous deciduous oaks, such as *Q. faginea/Q. pubescens*, are known to store a substantial amount of carbohydrates for the next year (Camarero et al., 2016) and most of their stem hydraulic conductivity depends on the wide earlywood vessels formed before the leaf unfolding (Sass-Klaassen et al., 2011). This exposes ring-porous broadleaved trees with large vessels to cavitation risks caused by negative water potential during dry summer days (Meinzer et al., 2010). Attenuation of photosynthesis rate (Resco de Dios et al., 2020) and partial or total leaf shedding of deciduous oaks during dry summer also prevent them to effectively increase radial growth in the response to autumn rains. By contrast, evergreen diffuse-porous species, like *Q. ilex*, show lower cavitation risk related to smaller vessels. Thanks to the elevated conductivity in the outermost rings of the sapwood, larger pools of carbohydrates (Camarero et al., 2016; Corcuera et al., 2004a) and permanent leaves they can reactivate photosynthesis faster after seasonal quiescence. Consequently, *Q. faginea* is considered to be a more drought-sensitive species compared with *Q. ilex* (Corcuera et al., 2004a, 2004b). This is supported by available species distribution models that forecast a decline of *Q. faginea* and an expansion of *Q. ilex* across the Iberian Peninsula with ongoing climate change (López-Tirado and Hidalgo, 2018). Our observations and simulations of higher growth bimodality in *Q. ilex* corroborate a physiological adaptations of this species to better overcome climate change in the Mediterranean region.

4.3. The VS-model performance

The VS-model with daily simulations provided longer and finer overview of intra-annual growth patterns compared with empirical dendrometer and xylogenesis monitoring performed during single year in biweekly interval. Although the model was initially developed for conifers from cold environments with short growing seasons (Vaganov et al., 2006), our results support its applicability also for Mediterranean

broadleaves. A highly significant correlations between simulated and observed regional master chronologies ($r = 0.82$–0.83) suggest that the model precisely captured regional climate-growth responses. Systematically higher correlations obtained for site chronologies of *Q. faginea/Q. pubescens* compared with *Q. ilex* might be linked to higher sensitivity to environmental variation (Fig. S7; Camarero et al., 2016) and higher correlation among individual tree-ring width series (Table S1) of the former compared with the later species. Similarly, the higher correlations in inland sites compared with coastal sites (Fig. 1a) might be due to the higher complexity of soil moisture dynamics in maritime areas with a bimodal precipitation compared with continental areas with less autumn precipitation and a marked dry summer (Knoben et al., 2019).

The VS-model simulations and linear climate-growth correlations confirmed drought limitation of growth during spring and summer for both species. By contrast, correlations did not fully capture the effects of autumn precipitation on radial growth as indicated by non-significant correlation coefficients at most sites (Fig. S7). The insufficient ability of linear models to reflect the importance of autumn growth conditions was previously observed even for a tree species with strongly bimodal growth, such as *P. halepensis* (de Luis et al., 2013; Tumajer et al., 2021b). The second growth period in autumn, albeit ecologically very important in seasonally dry environments (Mitrakos, 1980), usually represents less than 20% (Zhang et al., 2020) and only rarely reaches 50% (Campelo et al., 2007) of the annual tree-ring width. Consequently, the overall contribution of autumn growth rates to inter-annual variability of tree-ring widths is marginal. Therefore, the relevance of autumn growth for broadleaves might not be significantly reflected by linear models correlating annual ring widths with monthly or seasonal climatic variables. This highlights the relevance of non-linear process-based models operating on a daily scale as suitable tools accounting for the ecological importance of growth bimodality in seasonally-dry Mediterranean conditions. Further intra-annual growth records, mainly from subdaily (automatic dendrometers) to biweekly (xylogenesis) scales, are needed for Mediterranean forests to enable proper calibration of process-based models.

5. Conclusions

The combination of the growth modeling and stem radial increment monitoring revealed both spatial and species-specific differences in the growth patterns of the coexisting Mediterranean oak species with two contrasting life strategies. The highest intensity of growth bimodality was observed at Mediterranean coastal sites with a marked autumn precipitation peak following a summer drought. Moreover, simulated and observed intra-annual growth showed more significant bimodality for evergreen *Q. ilex* in comparison with deciduous *Q. faginea/Q. pubescens* at the Mediterranean sites. These differences in intra-annual growth plasticity might determine a differential response of oak species to past and future climate change and might influence future growth projections across the Mediterranean region. Future applications of both direct and indirect approaches to assess intra-annual growth dynamics are recommended for other seasonally dry regions and species to improve forecasts of dry forests' responses to climate change.

Declaration of Competing Interest

All authors declare that they have no conflicts of interest.

Data availability

Data will be made available on request.

Acknowledgements

Supplementary materials

Supplementary material associated with this article can be found, in the online version, at doi:10.1016/j.agrformet.2022.109234.

References

Alday, J.G., Camarero, J.J., Revilla, J., Resco de Dios, V., 2020. Similar diurnal, seasonal and annual rhythms in radial root expansion across two coexisting Mediterranean oak species. Tree Physiol 40, 956–968. https://doi.org/10.1093/treephys/tpaa041.

Babst, F., Bouriaud, O., Poulter, B., Trouet, V., Girardin, M.P., Frank, D.C., 2019. Twentieth century redistribution in climatic drivers of global tree growth. Sci. Adv. 5, eaat4313. https://doi.org/10.1126/sciadv.aat4313.

Balzano, A., Balzano, A., De Micco, V., 2018. Wood-trait analysis to understand climatic factors triggering intra-annual density-fluctuations in co-occurring Mediterranean trees. IAWA J. https://doi.org/10.1163/22941932-40190220.

Bunn, A.G., 2008. A dendrochronology program library in R (dplR). Dendrochronologia 26, 115–124. https://doi.org/10.1016/J.DENDRO.2008.01.002.

Camarero, J.J., Olano, J.M., Parras, A., 2010. Plastic bimodal xylogenesis in conifers from continental Mediterranean climates. New Phytol. 185, 471–480. https://doi.org/10.1111/j.1469-8137.2009.03073.x.

Camarero, J.J., Rubio-Cuadrado, Á., Gazol, A., 2021. Climate windows of intra-annual growth and post-drought recovery in Mediterranean trees. Agric. For. Meteorol. 108606, 308–309. https://doi.org/10.1016/j.agrformet.2021.108606.

Camarero, J.J., Sangüesa-Barreda, G., Vergarechea, M., 2016. Prior height, growth, and wood anatomy differently predispose to drought-induced dieback in two Mediterranean oak species. Ann. For. Sci. 73, 341–351. https://doi.org/10.1007/s13595-015-0523-4.

Campelo, F., Gutiérrez, E., Ribas, M., Nabais, C., Freitas, H., 2007. Relationships between climate and double rings in Quercus ilex from northeast Spain. Can. J. For. Res. 37, 1915–1923. https://doi.org/10.1139/X07-050.

Campelo, F., Gutiérrez, E., Ribas, M., Sánchez-Salguero, R., Nabais, C., Camarero, J.J., 2018. The facultative bimodal growth pattern in Quercus ilex – a simple model to predict sub-seasonal and inter-annual growth. Dendrochronologia 49, 77–88. https://doi.org/10.1016/j.dendro.2018.03.001.

Campelo, F., Ribas, M., Gutiérrez, E., 2021. Plastic bimodal growth in a Mediterranean mixed-forest of Quercus ilex and Pinus halepensis. Dendrochronologia 67, 125836. 10.1016/j.dendro.2021.125836.

Caudullo, G., Welk, E., San-Miguel-Ayanz, J., 2017. Chorological maps for the main European woody species. Data Br. 12, 662–666. https://doi.org/10.1016/j.dib.2017.05.007.

Cherubini, P., Gartner, B.L., Tognetti, R., Bräker, O.U., Schoch, W., Innes, J.L., 2003. Identification, measurement and interpretation of tree rings in woody species from mediterranean climates. Biol. Rev. Camb. Philos. Soc. 78, 119–148. https://doi.org/10.1017/S1464793102006000.

Coll, L., Camarero, J.J., Martínez De Aragón, J., 2012. Fine root seasonal dynamics, plasticity, and mycorrhization in 2 coexisting Mediterranean oaks with contrasting aboveground phenology. Écoscience 19, 238–245. https://doi.org/10.2980/19-3-3488.

Cook, E.R., Peters, K., 1981. The smoothing spline: a new approach to standardizing forest interior tree-ring width series for dendroclimatic studies. Tree-Ring Bull. 41, 45–53.

Corcuera, L., Camarero, J.J., Gil-Pelegrín, E., 2004a. Effects of a severe drought on Quercus ilex radial growth and xylem anatomy. Trees Struct. Funct. 18, 83–92. https://doi.org/10.1007/s00468-003-0284-9.

Corcuera, L., Camarero, J.J., Gil-Pelegrín, E., 2004b. Effects of a severe drought on growth and wood anatomical properties of Quercus faginea. IAWA J. 25, 185–204. https://doi.org/10.1163/22941932-90000360.

Cornes, R.C., van der Schrier, G., van den Besselaar, E.J.M., Jones, P.D., 2018. An ensemble version of the E-OBS temperature and precipitation data sets. J. Geophys. Res. Atmos. 123, 9391–9409. https://doi.org/10.1029/2017JD028200.

Cuny, H.E., Rathgeber, C.B.K., Frank, D., Fonti, P., Mäkinen, H., Prislan, P., Rossi, S., del Castillo, E.M., Campelo, F., Vavrčík, H., Camarero, J.J., Bryukhanova, M.V., Jyske, T., Gričar, J., Gryc, V., De Luis, M., Vieira, J., Čufar, K., Kirdyanov, A.V., Oberhuber, W., Treml, V., Huang, J.-G., Li, X., Swidrak, I., Deslauriers, A., Liang, E., Nöjd, P., Gruber, A., Nabais, C., Morin, H., Krause, C., King, G., Fournier, M., 2015. Woody biomass production lags stem-girth increase by over one month in coniferous forests. Nat. Plants 1, 15160. https://doi.org/10.1038/nplants.2015.160.

de Luis, M., Čufar, K., Di Filippo, A., Novak, K., Papadopoulos, A., Piovesan, G., Rathgeber, C.B.K., Raventós, J., Saz, M.A., Smith, K.T., 2013. Plasticity in Dendroclimatic response across the distribution range of aleppo pine (Pinus halepensis). PLoS ONE 8, e83550. https://doi.org/10.1371/journal.pone.0083550.

de Luis, M., Gričar, J., Čufar, K., Raventós, J., 2007. Seasonal dynamics of wood formation in pinus halepensis from dry and semi-arid ecosystems in Spain. IAWA J. 28, 389–404. https://doi.org/10.1163/22941932-90001651.

De Micco, V., Balzano, A., Čufar, K., Aronne, G., Gričar, J., Merela, M., Battipaglia, G., 2016. Timing of false ring formation in Pinus halepensis and arbutus Unedo in southern Italy: outlook from an analysis of xylogenesis and tree-ring chronologies. Front. Plant Sci. 7, 1–14. https://doi.org/10.3389/fpls.2016.00705.

Delpierre, N., Lireux, S., Hartig, F., Camarero, J.J., Cheaib, A., Čufar, K., Cuny, H., Deslauriers, A., Fonti, P., Gričar, J., Huang, J., Krause, C., Liu, G., de Luis, M., Mäkinen, H., Martinez del Castillo, E., Morin, H., Nöjd, P., Oberhuber, W., Prislan, P., Rossi, S., Saderi, S., Treml, V., Vavrick, H., Rathgeber, C.B.K., 2019. Chilling and forcing temperatures interact to predict the onset of wood formation in Northern Hemisphere conifers. Glob. Change Biol. 25, 1089–1105. https://doi.org/10.1111/gcb.14539.

Drew, D.M., Downes, G.M., 2009. The use of precision dendrometers in research on daily stem size and wood property variation: a review. Dendrochronologia 27, 159–172. https://doi.org/10.1016/j.dendro.2009.06.008.

Eckes-Shephard, A.H., Ljungqvist, F.C., Drew, D.M., Rathgeber, C.B.K., Friend, A.D., 2022. Wood formation modeling – a research review and future perspectives. Front. Plant Sci. 13, 265. https://doi.org/10.3389/fpls.2022.837648.

Evans, M.N., Reichert, B.K., Kaplan, A., Anchukaitis, K.J., Vaganov, E.A., Hughes, M.K., Cane, M.A., 2006. A forward modeling approach to paleoclimatic interpretation of tree-ring data. J. Geophys. Res. 111, G03008. https://doi.org/10.1029/2006JG000166.

Gärtner, H., Schweingruber, F.H., 2013. Microscopic Preparation Techniques for Plant Stem Analysis. Verlag Dr. Kessel, Remagen-Oberwinter.

Gazol, A., Camarero, J.J., Vicente-Serrano, S.M., Sánchez-Salguero, R., Gutiérrez, E., de Luis, M., Sangüesa-Barreda, G., Novak, K., Rozas, V., Tíscar, P.A., Linares, J.C., Martín-Hernández, N., Martínez del Castillo, E., Ribas, M., García-González, I., Silla, F., Camisón, A., Génova, M., Olano, J.M., Longares, L.A., Hevia, A., Tomás-Burguera, M., Galván, J.D., 2018. Forest resilience to drought varies across biomes. Glob. Chang Biol. 24, 2143–2158. https://doi.org/10.1111/gcb.14082.

Hastie, T., 2022. Gam: Generalized additive models. R package version 1.20.2.

Holmes, R.L., 1983. Computer-assisted quality control in tree-ring dating and measurement. Tree-Ring Bull. 43, 69–78.

Huang, J.-G., Ma, Q., Rossi, S., Biondi, F., Deslauriers, A., Fonti, P., Liang, E., Mäkinen, H., Oberhuber, W., Rathgeber, C.B.K., Tognetti, R., Treml, V., Yang, B., Zhang, J.-L., Antonucci, S., Bergeron, Y., Camarero, J.J., Campelo, F., Čufar, K., Cuny, H.E., De Luis, M., Giovannelli, A., Gričar, J., Gruber, A., Gryc, V., Güney, A., Guo, X., Huang, W., Jyske, T., Kašpar, J., King, G., Krause, C., Lemay, A., Liu, F., Lombardi, F., Martinez del Castillo, E., Morin, H., Nabais, C., Nöjd, P., Peters, R.L., Prislan, P., Saracino, A., Swidrak, I., Vavrčík, H., Vieira, J., Yu, B., Zhang, S., Zeng, Q., Zhang, Y., Ziaco, E., 2020. Photoperiod and temperature as dominant environmental drivers triggering secondary growth resumption in Northern Hemisphere conifers. Proc. Natl. Acad. Sci. 117, 20645–20652. https://doi.org/10.1073/pnas.2007058117.

Huang, L., Xue, W., Herben, T., 2019. Temporal niche differentiation among species changes with habitat productivity and light conditions. J. Veg. Sci. 30, 438–447. https://doi.org/10.1111/jvs.12741.

Jevšenak, J., Levanič, T., 2018. dendroTools: r package for studying linear and nonlinear responses between tree-rings and daily environmental data. Dendrochronologia 48, 32–39. https://doi.org/10.1016/j.dendro.2018.01.005.

Knoben, W.J.M., Woods, R.A., Freer, J.E., 2019. Global bimodal precipitation seasonality: a systematic overview. Int. J. Climatol. 39, 558–567. https://doi.org/10.1002/joc.5786.

López-Tirado, J., Hidalgo, P.J., 2018. Predicting suitability of forest dynamics to future climatic conditions: the likely dominance of Holm oak [Quercus ilex subsp. ballota (Desf.) Samp.] and Aleppo pine (Pinus halepensis Mill.). Ann. For. Sci. 75 https://doi.org/10.1007/s13595-018-0702-1.

Martínez-Sancho, E., Gutiérrez, E., Valeriano, C., Ribas, M., Popkova, M.I., Shishov, V.V., Dorado-Liñán, I., 2021. Intra- and inter-annual growth patterns of a mixed pine-oak forest under mediterranean climate. Forests 12, 1746. https://doi.org/10.3390/f12121746.

Meinzer, F.C., McCulloh, K.A., Lachenbruch, B., Woodruff, D.R., Johnson, D.M., 2010. The blind men and the elephant: the impact of context and scale in evaluating conflicts between plant hydraulic safety and efficiency. Oecologia 164, 287–296. https://doi.org/10.1007/s00442-010-1734-x.

Meyer, D., Dimitriadou, E., Hornik, K., Weingessel, A., Leisch, F., 2021. e1071: misc functions of the department of statistics. Probab. Theory Group (Formerly: E1071).

Mitrakos, K.A., 1980. A theory for mediterranean plant life. Acta Oecol. 1, 245–252.

Montserrat-Martí, G., Camarero, J.J., Palacio, S., Pérez-Rontomé, C., Milla, R., Albuixech, J., Maestro, M., 2009. Summer-drought constrains the phenology and

growth of two coexisting Mediterranean oaks with contrasting leaf habit: implications for their persistence and reproduction. Trees 23, 787–799. https://doi.org/10.1007/s00468-009-0320-5.

Morino, K., Minor, R.L., Barron-Gafford, G.A., Brown, P.M., Hughes, M.K., 2021. Bimodal cambial activity and false-ring formation in conifers under a monsoon climate. Tree Physiol. 41, 1893–1905. https://doi.org/10.1093/treephys/tpab045.

Pacheco, A., Camarero, J.J., Ribas, M., Gazol, A., Gutierrez, E., Carrer, M., 2018. Disentangling the climate-driven bimodal growth pattern in coastal and continental Mediterranean pine stands. Sci. Total Environ. 615, 1518–1526. https://doi.org/10.1016/j.scitotenv.2017.09.133.

Pan, Y., Birdsey, R.A., Fang, J., Houghton, R., Kauppi, P.E., Kurz, W.A., Phillips, O.L., Shvidenko, A., Lewis, S.L., Canadell, J.G., Ciais, P., Jackson, R.B., Pacala, S.W., McGuire, A.D., Piao, S., Rautiainen, A., Sitch, S., Hayes, D., 2011. A large and persistent carbon sink in the world's forests. Science 333 (80-), 988–993. https://doi.org/10.1126/science.1201609.

Peguero-Pina, J.J., Sancho-Knapik, D., Barrón, E., Camarero, J.J., Vilagrosa, A., Gil-Pelegrín, E., 2014. Morphological and physiological divergences within Quercus ilex support the existence of different ecotypes depending on climatic dryness. Ann. Bot. 114, 301–313. https://doi.org/10.1093/aob/mcu108.

Peñuelas, J., Rutishauser, T., Filella, I., 2009. Phenology feedbacks on climate change. Science 324 (80-), 887–888. https://doi.org/10.1126/science.1173004.

Popkova, M.I., Vaganov, E.A., Shishov, V.V., Babushkina, E.A., Rossi, S., Fonti, M.V., Fonti, P., 2018. Modeled tracheidograms disclose drought influence on pinus sylvestris tree-rings structure from siberian forest-steppe. Front. Plant Sci. 9, 1144. https://doi.org/10.3389/fpls.2018.01144.

Prislan, P., Gričar, J., de Luis, M., Novak, K., Martinez del Castillo, E., Schmitt, U., Koch, G., Štrus, J., Mrak, P., Žnidarič, M.T., Čufar, K., 2016. Annual cambial rhythm in pinus halepensis and pinus sylvestris as indicator for climate adaptation. Front. Plant Sci. 7, 1–15. https://doi.org/10.3389/fpls.2016.01923.

R Core Team, 2021. R: A Language and Environment For Statistical Computing (version 4.1.2.). R Foundation for Statistical Computing, Vienna, Austria.

Rathgeber, C.B.K., Cuny, H.E., Fonti, P., 2016. Biological basis of tree-ring formation: a crash course. Front. Plant Sci. 7, 1–7. https://doi.org/10.3389/fpls.2016.00734.

Resco de Dios, V., Arteaga, C., Peguero-Pina, J.J., Sancho-Knapik, D., Qin, H., Zveushe, O.K., Sun, W., Williams, D.G., Boer, M.M., Voltas, J., Moreno, J.M., Tissue, D.T., Gil-Pelegrín, E., 2020. Hydraulic and photosynthetic limitations prevail over root non-structural carbohydrate reserves as drivers of resprouting in two Mediterranean oaks. Plant. Cell Environ. 43, 1944–1957. https://doi.org/10.1111/pce.13781.

Rossi, S., Anfodillo, T., Menardi, R., 2006. Trephor: a new tool for sampling microcores from tree stems. IAWA J. 27, 89–97. https://doi.org/10.1163/22941932-90000139.

Sass-Klaassen, U., Sabajo, C.R., den Ouden, J., 2011. Vessel formation in relation to leaf phenology in pedunculate oak and European ash. Dendrochronologia 29, 171–175. https://doi.org/10.1016/j.dendro.2011.01.002.

Shishov, V.V., Tychkov, I.I., Popkova, M.I., Ilyin, V.A., Bryukhanova, M.V., Kirdyanov, A. V., 2016. VS-oscilloscope: a new tool to parameterize tree radial growth based on climate conditions. Dendrochronologia 39, 42–50. https://doi.org/10.1016/j.dendro.2015.10.001.

Soja, A.J., Tchebakova, N.M., French, N.H.F., Flannigan, M.D., Stocks, B.J., Sukhinin, A. I., Parfenova, E.I., Chapin, F.S., Stackhouse, P.W., 2007. Climate-induced boreal

forest change: predictions versus current observations. Glob. Planet. Change 56, 274–296. https://doi.org/10.1016/J.GLOPLACHA.2006.07.028.

Touchan, R., Shishov, V.V., Meko, D.M., Nouiri, I., Grachev, A., 2012. Process based model sheds light on climate sensitivity of Mediterranean tree-ring width. Biogeosciences 9, 965–972. https://doi.org/10.5194/bg-9-965-2012.

Tumajer, J., Buras, A., Camarero, J.J., Carrer, M., Shetti, R., Wilmking, M., Altman, J., Sangüesa-Barreda, G., Lehejček, J., Michaletz, S., 2021a. Growing faster, longer or both? Modelling plastic response of Juniperus communis growth phenology to climate change. Glob. Ecol. Biogeogr. 30, 2229–2244. https://doi.org/10.1111/geb.13377.

Tumajer, J., Shishov, V.V., Ilyin, V.A., Camarero, J.J., 2021b. Intra-annual growth dynamics of Mediterranean pines and junipers determines their climatic adaptability. Agric. For. Meteorol. 311, 108685 https://doi.org/10.1016/j.agrformet.2021.108685.

Tychkov, I.I., Sviderskaya, I.V., Babushkina, E.A., Popkova, M.I., Vaganov, E.A., Shishov, V.V., 2019. How can the parameterization of a process-based model help us understand real tree-ring growth? Trees 33, 345–357. https://doi.org/10.1007/s00468-018-1780-2.

Vaganov, E.A., Hughes, M.K., Shashkin, A.V., 2006. Growth Dynamics of Conifer Tree Rings: Images of Past and Future Environments, Ecological Studies. Springer-Verlag, Berlin/Heidelberg. https://doi.org/10.1007/3-540-31298-6.

Vieira, J., Campelo, F., Nabais, C., 2022. Environment controls seasonal and daily cycles of stem diameter variations in Portuguese oak (Quercus faginea Lambert). Forests 13. https://doi.org/10.3390/f13020170.

Vieira, J., Campelo, F., Nabais, C., 2017. Dendrochronology of maritime pine in the middle of the Atlantic Ocean. Dendrochronologia 45, 73–80. https://doi.org/10.1016/j.dendro.2017.06.009.

Wickham, H., 2009. ggplot2: Elegant Graphics For Data Analysis. Springer, Verlag-New York.

Wilmking, M., Maaten-Theunissen, M., Maaten, E., Scharnweber, T., Buras, A., Biermann, C., Gurskaya, M., Hallinger, M., Lange, J., Shetti, R., Smiljanic, M., Trouillier, M., 2020. Global assessment of relationships between climate and tree growth. Glob. Change Biol. 26, 3212–3220. https://doi.org/10.1111/gcb.15057.

Zalloni, E., de Luis, M., Campelo, F., Novak, K., De Micco, V., Di Filippo, A., Vieira, J., Nabais, C., Rozas, V., Battipaglia, G., 2016. Climatic signals from intra-annual density fluctuation frequency in mediterranean pines at a regional scale. Front. Plant Sci. 7, 1–11. https://doi.org/10.3389/fpls.2016.00579.

Zhang, J., Alexander, M.R., Gou, X., Deslauriers, A., Fonti, P., Zhang, F., Pederson, N., 2020. Extended xylogenesis and stem biomass production in Juniperus przewalskii Kom. during extreme late-season climatic events. Ann. For. Sci. 77, 99. https://doi.org/10.1007/s13595-020-01008-1.

Ziaco, E., Biondi, F., 2018. Stem circadian phenology of four pine species in naturally contrasting climates from sky-island forests of the western USA. Forests 9, 396. https://doi.org/10.3390/f9070396.

Zweifel, R., Haeni, M., Buchmann, N., Eugster, W., 2016. Are trees able to grow in periods of stem shrinkage? New Phytol. 211, 839–849. https://doi.org/10.1111/nph.13995.

Zweifel, R., Sterck, F., Braun, S., Buchmann, N., Eugster, W., Gessler, A., Häni, M., Peters, R.L., Walthert, L., Wilhelm, M., Ziemińska, K., Etzold, S., 2021. Why trees grow at night. New Phytol. 231, 2174–2185. https://doi.org/10.1111/nph.17552.